CHEMISTRY
A EUROPEAN JOURNAL

DOI: 10.1002/chem.200701324

Theoretical Studies of Damage to 3′-Uridine Monophosphate Induced by Electron Attachment

Ru bo Zhang,[a, b] Ke Zhang,[a] and Leif A. Eriksson*[b]

Abstract: Low-energy electrons (LEE) are well known to induce nucleic acid damage. However, the damage mechanisms related to charge state and structural features remain to be explored in detail. In the present work, we have investigated the N1-glycosidic and C3′–O(P) bond ruptures of 3′-UMP (UMP = uridine monophosphate) and the protonated form 3′-UMPH with −1 and zero charge, respectively, based on hybrid density functional theory (DFT) B3LYP together with the 6-31+G(d,p) basis set. The glycosidic bond breakage reactions of the 3′UMP and 3′UMPH electron adducts are exothermic in both cases, with barrier heights of 19–20 kcal mol^{-1} upon inclusion of bulk solvation. The effects of the charge state on the phosphate group are marginal, but the C2′–OH group destabilizes the transition structure of glycosidic bond rupture of 3′-UMPH in the gas phase by approximately 5.0 kcal mol^{-1}. This is in contrast with the C3′–O(P) bond ruptures induced by LEE in which the charge state on the phosphate influences the barrier heights and reaction energies considerably. The barrier towards C3′–O(P) bond dissociation in the 3′UMP electron adduct is higher in the gas phase than the one corresponding to glycosidic bond rupture and is dramatically influenced by the C2′–OH group and bulk salvation, which decreases the barrier to 14.7 kcal mol^{-1}. For the C3′–O(P) bond rupture of the 3′UMPH electron adduct, the reaction is exothermic and the barrier is even lower, 8.2 kcal mol^{-1}, which is in agreement with recent results for 3′-dTMPH and 5′-dTMPH (dTMPH = deoxythymidine monophosphate). Both the Mulliken atomic charges and unpaired-spin distribution play significant roles in the reactions.

Keywords: DNA damage · electron attachment · nucleobases · strand breakage · uridine

Introduction

The attachment of low-energy electrons (LEEs) to DNA has been addressed as a major cause of cellular damage.[1,2] The lesion reactions involve sugar phosphate C3′–O(P) and N1-glycosidic bond ruptures as well as loss of H atoms, the mechanisms of which have been proposed through recent experiments[3–17] and theoretical calculations.[18–33]

The mechanism of C3′–O(P) bond rupture (Scheme 1) in neutral 5′-dTMP (dTMP = deoxythymidine monophosphate) and 5′-dCMP (dCMP = deoxypcytidine monophosphate) models of DNA was suggested by Simons and co-workers[18–23] to proceed through the formation of a shape-resonance state—the LEE is captured in a π* orbital of a DNA base from which the rupture proceeds on the adiabatic surface. This is consistent with recent experimental results by Sanche and co-workers.[8] The sugar–phosphate–sugar

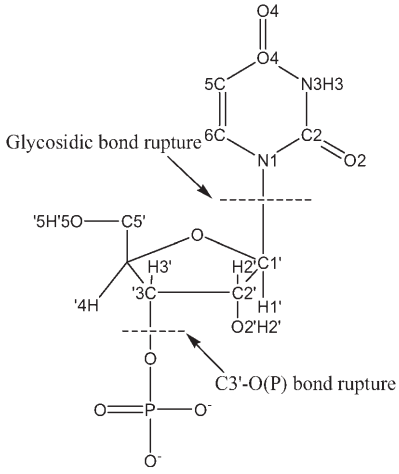

Scheme 1. The mechanism of C3′–O(P) bond rupture in neutral 5′-dTMP and 5′-dCMP models of DNA.

[a] Ass. Prof. R. b. Zhang, K. Zhang
School of Science and the Institute for Chemical Physics
Beijing Institute of Technology, Beijing 100081 (China)

[b] Ass. Prof. R. b. Zhang, Prof. L. A. Eriksson
Department of Natural Sciences and Örebro Life Science Center
Örebro University, 701 82 Örebro (Sweden)
E-mail: leif.eriksson@nat.oru.se

Supporting information for this article is available on the WWW under http://www.chemeurj.org/ or from the author.

system was also studied by Sevilla and co-workers[24] in which a dipole-bound LEE was attached to the model followed by a change to a valence-bound state in the transition structure. The barriers obtained for the sugar–phosphate bond cleavage processes were approximately 10 kcal mol^{-1}. Gu and co-workers[25–29] also calculated the barrier height of C3′−O(P) bond rupture by using a calibrated B3LYP/DZP++ theory. In their calculations, the LEE was initially attached to a π* orbital of a pyrimidine base and transferred to the C3′−O(P) σ bond at the transition state. Recent experimental findings by Konig et al.,[15] however, could not reproduce the results from Gu and co-workers' calculations and Sanche and co-workers' experiments, but showed that the mechanism of C3′−O (P) bond rupture is caused by the electrons that become attached directly to the phosphate group. Even more recently, Kumar and Sevilla[33] predicted the interaction of a LEE with 5′-dTMP at the B3LYP/6–31++G** level. The adiabatic and vertical anionic surfaces for C5′−O(P) bond rupture were calculated to have approximately the same barrier. Furthermore, the calculations supported the hypothesis of a transiently bound electron to a virtual orbital, which is likely to be crucial for C5′−O(P) bond rupture without significant molecular relaxation.

N1-glycosidic bond rupture (Scheme 1) of thymidine has been the focus in recent research by Sanche and co-workers[6] who showed that the LEE efficiently breaks the N-glycosidic bond of thymidine. The barriers in pyrimidine nucleosides (dT and dC) were estimated to be 17.6 and 20.4 kcal mol^{-1},[25] respectively, which are dramatically higher than that of C3′−O(P) rupture. As a result, the C3′−O(P) bond rupture was regarded as the main damage site, leading to DNA strand break.

As discussed above, only LEE-induced DNA strand breakage in neutral pyrimidines have been calculated as the neutral species possess positive electron affinities and pyrimidine bases can capture an excess electron to form a stable anionic state. When a partially negative phosphate group and the reduced nucleotide are present simultaneously in DNA, electron transfer can occur and may also be influenced by the local degree of hydration. As RNA has almost the same chemical functional groups and structure as single-stranded DNA, a rational deduction can be made that LEE should also lead to RNA strand breakage. RNA carries a C2′−OH group close to the 3′-phosphate, whose importance has been recognized in RNA catalytic mechanisms.[34] However, the details of the LEE-damaged RNA are still not clear, especially the effects of the C2′−OH group and the charge state of the phosphate group on lesion formation, which are still to be elucidated. Herein, we attempt to address some of these issues. Two models, 3′-UMP (**U**) and the protonated form 3′-UMPH (**UH**; UMP = uridine monophosphate) and their electron adducts (•**U** and •**UH**) are studied by theoretically assuming an adiabatic approximation (see Scheme 1). We can further assume that the models should have similar structures and properties as 3′-dTMP and its neutral (protonated) species. Atomic labeling of the models used in this work is given in Scheme 1.

Methodology

The geometries of 3′UMP, 3′UMPH, and their electron adducts were optimized at the hybrid density functional theory level B3LYP[35,36] in conjunction with the 6-31+G(d,p) basis set. Frequency calculations were also performed to confirm the correct nature of the stationary points and to extract the zero-point vibrational effects (ZPE) and estimates of the free energy at 298 K. For the glycosidic bond rupture processes, the potential-energy surfaces (PES) were scanned from the initial electron adducts by varying the N1−C1′ distance by using a step length of 0.1 Å and optimizing the remaining coordinates. The same procedure was used to determine the PES of C3′−O(P) bond dissociation of the electron adducts by scanning C3′−O(P) distance. The Mulliken charges and unpaired spin densities were determined throughout the dissociation processes. The structures at the highest energy points along the scanned PESs were used as the input for full transition-state optimizations, from which intrinsic reaction coordinate calculations were performed to verify that the TSs were connected to the correct reactants and products. Bulk solvation effects were considered by using the integral electron formalism of the polarized continuum model (IEF-PCM)[37] with a dielectric constant of 78.4. All calculations were carried out by using the Gaussian 03 package.[38] To verify the trends, single-point calculations were also performed at the B3LYP/DZP++ level.

Results and Discussion

Structures of neutral and reduced 3′UMP and 3′UMPH: Geometries of the 3′UMP (**U**) and 3′UMPH (**UH**) electron adducts (labeled •**U** and •**UH**, respectively) were optimized at the B3LYP/6-31+G(d,p) level. The geometries of the corresponding parent molecules **U** and **UH** were also optimized at the same level of theory. Figure 1 illustrates the distances between the atoms of interest in the initial complexes, the transition structures, and the final structures in the bond-breaking processes studied.

In **U**, the C5−C6, N1−C1′, and C3′−O(P) bond lengths are 1.355, 1.466, and 1.417 Å, respectively. When an excess electron is added, the C5−C6 bond length is extended to 1.424 Å, which is intermediate between C−C single- and double-bond lengths. The C3′−O(P) distance is slightly elongated, around 0.02 Å, and the N1−C1′ distance is essentially unchanged by the electron addition. O2′−H2′···O(P) hydrogen bonding is present with a distance of 1.934 Å in **U**, which is slightly extended compared with the distance of 2.106 Å in •**U**. In addition, owing to the interaction of the excess electron with uracil, the C6 site becomes pyramidal, as seen through the angles C5-C6-N1 + C5-C6-H6 + H6-C6-N1 = 349.0°. The O5′−H5′···C6 distance becomes 2.189 Å, which is characteristic of a σ-type hydrogen bonding.

For **UH**, in which the phosphate group is neutralized by two hydrogen atoms, the C5−C6, N1−C1′ bond lengths are almost identical to those of **U**. The C3′−O(P) bond length,

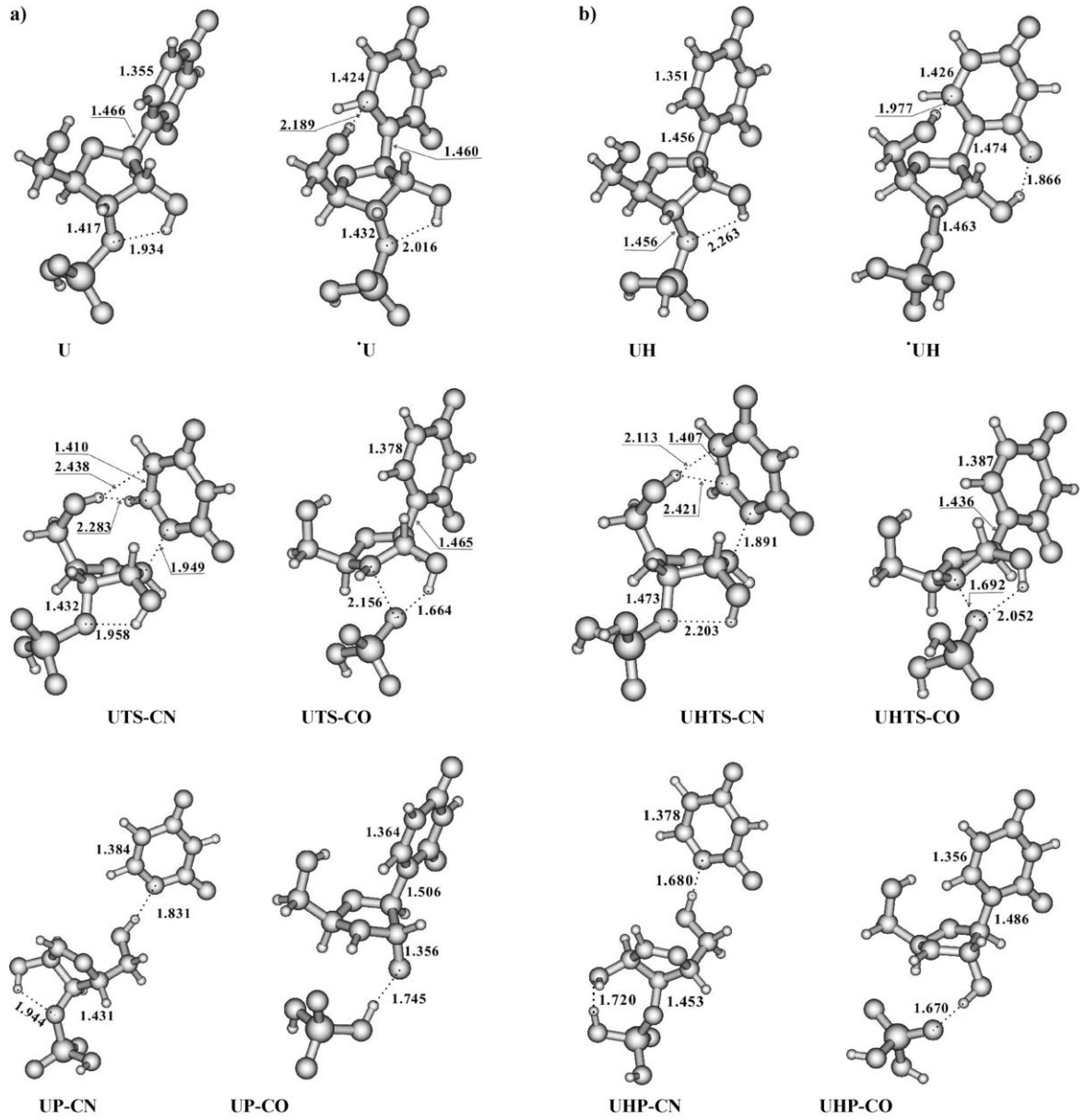

Figure 1. Selected geometrical parameters (B3LYP/6-31+G(d,p) level) of the stationary structures along the N1-glycosidic and C3′–O(P) bond rupture reactions of a) •**U** and b) •**UH**.

however, is increased by approximately 0.04 Å. The O2′–H2′···O(P) distance is elongated to 2.263 Å, showing that the basicity of O(P) is lowered. In •**UH**, the C5–C6 bond length increases to 1.426 Å, which is almost equal to the one in •**U**. The bond lengths of N1–C1′ and C3′–O(P) in **UH** are larger than those in •**U** by 0.01 Å and 0.03 Å, respectively. Interestingly, O2′–H2′···O2 hydrogen bonding is observed in **UH** (as opposed to •**U**), which implies that the basicity of O(P) is lowered further and that of O2 is raised owing to electron addition in **UH**. The pyramidal C6 site is also observed in •**UH**.

The singly occupied molecular orbitals (SOMO) and lowest unoccupied molecular orbitals (LUMO) of the radical systems are displayed in Figure 2. For •**U** and •**UH**, the SOMOs are exclusively populated on the uracil base, which results in the higher electronegativity on the base. Thus, the strength and connectivity of the hydrogen bond involving O2′–H2′ varies with the protonation state of the phosphate group and the electron addition. In contrast, the shape of the LUMOs of •**U** and •**UH** is significantly different as it is not localized on the uracil base of •**U**, but on the phosphate group of •**UH**.

During the glycosidic bond-breaking process, the C3′–O(P) bond length remains unchanged compared with the initial electron adduct. At the transition state (**UTS-CN**), the pyramidality at the C6 site is reduced and the C5–C6 distance becomes 1.410 Å. An OH···π interaction is formed with the O5′–H5′ distances to C5 and C6 being 2.438 and

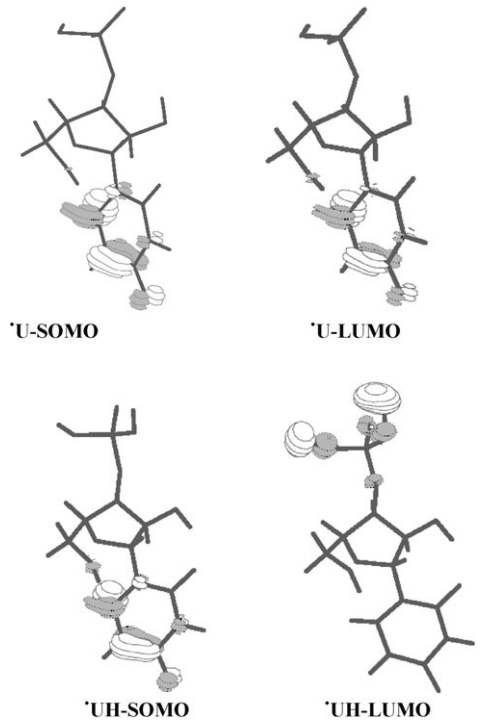

Figure 2. SOMO and LUMO populations of **•U** (top row) and **•UH** (bottom row).

2.283 Å, respectively. This is quite different from the results by Gu and co-workers,[25] which show a close distance between O5′–H5′ and N1 in deoxythymine (dT) and deoxycytosine (dC). At the same time, the O2′−H2′···O(P) hydrogen bond is contracted to 1.958 Å. The N1···C1′ distance is 1.949 Å and the related imaginary frequency is $512i\ cm^{-1}$, which describes the N1−C1′ bond breakage. For **UHTS-CN** (see Figure 1b), similar changes are also observed. The N1···C1′ distance is 1.891 Å and its corresponding imaginary frequency is $521i\ cm^{-1}$. In addition, the O2′−H2′···O(P) hydrogen bonding is reformed with a distance of 2.203 Å. For the final products, the relative orientation of the two separate fragments—uracil base and ribose + phosphate group—change dramatically compared with the initial electron adducts and are connected through N1···H5′ hydrogen bonds with distances of 1.831 Å in **UP-CN** and 1.680 Å in **UHP-CN**. The O2′−H2′···O(P) distance is 1.944 Å in **UP-CN** and hence weakened, whereas in **UHP-CN**, a O2′···HO(P) hydrogen bond is formed with a distance of 1.720 Å.

The alternative competing process—C3′−O(P) bond rupture—has been explored at the same level of theory. For the **UTS-CO** state, the C5−C6 and N1−C1′ distances approach the corresponding values found in **U** and the interaction between O5′H5′ and the uracil base disappears. The C3′···O(P) distance is 2.156 Å, which is considerably longer than the value in **UHTS-CO** (1.692 Å). The imaginary frequencies $345i\ cm^{-1}$ in **UTS-CO** and $818i\ cm^{-1}$ in **UHTS-CO** both correspond to C3′−O(P) bond ruptures. The neighboring O2′−H2′ starts forming hydrogen bonds with the leaving phosphate group in the transition states, with distances 1.664 Å in **UTS-CO** and 2.052 Å in **UHTS-CO**. In the corresponding products, H2′ displays a completely different behavior. In **UP-CO**, H2′ is transferred without any barrier to O from the phosphate group (see the Supporting Information), and the H2′···O2′ distance is 1.745 Å. In **UHP-CO**, on the other hand, H2′ remains bound to O2′ and hydrogen bonds to O(P) with a distance of 1.670 Å are formed.

Energetic profiles of glycosidic and C3′−O(P) bond ruptures: *Electron affinities*: The electron affinities of 3′UMP and 3′UMPH are presented in Table 1. In the gas phase, **U** becomes unstable when it captures an excess electron, showing that it is an endothermic process. The vertical and adiabatic electron affinities (VEA and AEA) of **U** are −2.26 and −1.77 eV with ZPE correction, respectively. The vertical detachment energy (VDE) is calculated to −0.69 eV, showing that the adiabatic dianion is unstable in the gas phase. They do, however, become positive under the influence of bulk solvation, indicating that the electron adduct is stabilized in polar solution. **UH**, on the other hand, can capture an excess electron exothermically with the corresponding gas phase VEA and AEA being positive (+0.14 eV and +0.62 eV, respectively). The VDE is, as expected, also positive (+1.72 eV), indicating that the anion radical can be stable in the gas phase. The values are comparable with those for 3′-dTMPH (0.26 eV (VEA), 0.56 eV (AEA), and 1.53 eV (VDE)), which were obtained at the B3LYP/DZP++ level,[25] and 5′-dTMPH (0.40 eV (AEA) and 0.97 eV (VDE)), which were predicted at the B3LYP/6–31++G-(d,p) level.[33] Bulk solvation increases the above values of **•UH** such that the VDE is 3.12 eV in aqueous solution, which is comparable with the value of 3.04 eV found for of **•U** under the same conditions. Thus the negative charge on the phosphate group appears not to be a barrier to attachment of an excess electron within the bulk solvation approximation. The added electron is entirely localized on the uracil base in **•U** (see Figure 2), which helps to stabilize the negatively charged centers by the solvation.

Table 1. Vertical (VEA), adiabatic (AA) electron affinities, and vertical (VDE)[a] detachment energies (eV) of 3′UMP and 3′UMPH in the gas phase and bulk solvation ($\varepsilon = 78.4$).

	VEA[b]	AEA[c]	VDE[b]
•U	−1.77		
	−2.26	−1.88	−0.69
	1.68[d]	2.06	3.04
•UH		0.71	
	0.14	0.62 (0.18)[e]	1.72
	1.65[d]	2.09	3.12

[a] The definitions of VEA, AEA, and VDE are as in reference [39]. [b] No ZPE value included. [c] ZPE values are included. [d] In bulk solvation. [e] The AEA value in reference [40].

N1-glycosidic bond rupture: The stabilities of N1-glycosidic bonds in the electron adducts of 3′-UMP and 3′-UMPH are

presented in Table 2 and Figure 3. The barrier heights of glycosidic bond breakage in **•U** are 23.0 and 21.0 kcal mol^{-1} with ZPE correction. The current results are similar to the values 18.9 kcal mol^{-1} for dT and 21.6 kcal mol^{-1} for dC, which were reported by Gu et al.[25] in which the effects of a negative charge on the phosphate was not considered. To explore the role of the C2′-OH group, the mutant in which C2′-OH is replaced by H in **•U** was also optimized. The barrier height found is slightly reduced, yet it is still comparable with the parent system. Including bulk solvation effects in the parent system leads to a barrier of 19.1 kcal mol^{-1} including ZPE correction. The corresponding activation free-energy change at 298 K is 20.1 kcal mol^{-1}. The reaction energy is −17.5 and −21.9 kcal mol^{-1} with thermal corrections at 298 K in the gas phase, which shows that the process of glycosidic bond rupture in **•U** is exothermic.

Table 2. B3LYP/6-31+G(d,p) reaction energies and activation barriers (in kcal mol^{-1}) for the N1-glycosidic and C3′−O(P) bond-breakage reactions.

	Scission of N1−C1′ bond		Scission of C3′−O(P) bond	
	ΔE^{+}	ΔE	ΔE^{+}	ΔE
•U	23.0 (22.4)[d] (23.8)[e] (21.9)[f]	−15.6	32.0 (44.9) (32.7) (17.9)	17.8
[a]	21.0 (20.4)[d]	−17.5	29.6 (42.5)	15.3
[b]	19.1	−11.4	14.7	1.0
[c]	20.1	−21.9	28.7	13.4
•UH	25.9 (20.6)[d] (26.5)[e] (23.0)[f]	−16.7	10.7 (9.5) (11.1) (13.1)	−27.6
[a]	23.6 (18.6)[d]	−17.8	8.2 (7.1)	−28.7
[b]	20.0	−13.7	10.3	−24.2
[c]	23.0	−20.3	6.8	−31.4

[a] ZPE values included. [b] ZPE corrections and bulk solvation effects included. [c] Free-energy barrier at T = 298 K. [d] Values in parenthesis corresponding to the systems with C2′-OH replaced by H atom. [e] The values are obtained by B3LYP/DZP++ with no ZPE included. [f] In bulk solvation, the values are obtained by B3LYP/DZP++ with no ZPE included.

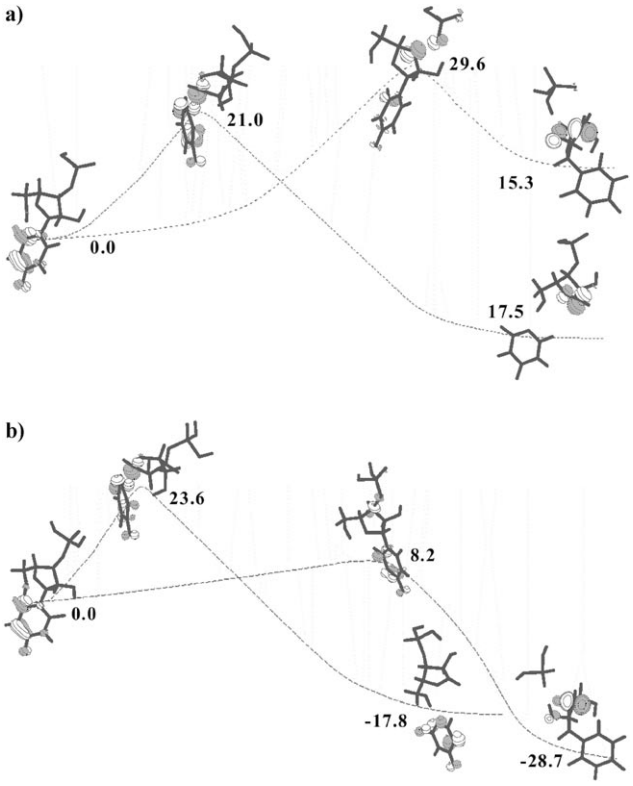

Figure 3. ZPE-corrected energy profiles (in kcal mol^{-1}) corresponding to the N1-glycosidic and C3′−O(P) bond breakage reactions in a) **•U** and b) **•UH**, computed at the B3LYP/6-31+G(d,p) level.

According to the above results, glycosidic bond rupture in **•U** and **•UH** is exothermic with high associated transition barriers in the gas phase and moderate ones in aqueous solution. Protonation of the phosphate group increases the stability of the transition-state structures. The C2′−OH group is found to destabilize the transition structures, especially that of **UHTS-CN**. Bulk solvation can lower the barriers by as much as 3 kcal mol^{-1}.

C3′−O(P) rupture: An alternative form of damage to **•U** and **•UH** is that of C3′−O(P) breakage, which leads to strand break. For the process to occur in **•U**, a barrier height of 32.0 kcal mol^{-1} (29.6 kcal mol^{-1} with ZPE correction) must be overcome in the gas phase. This is considerably higher than what was found for glycosidic bond rupture. The reaction energy is strongly positive. Strikingly, bulk solvation reduces the barrier height by up to 14.7 kcal mol^{-1} and leads to an essentially thermoneutral reaction (reaction energy 1.0 kcal mol^{-1}). With the replacement of C2′−OH by H, the barrier is drastically increased up to 42.5 kcal mol^{-1} with ZPE correction, which shows that C2′−OH contributes significantly to the stabilization of the transition state. For this system, we can conclude that glycosidic bond rupture is the major pathway in the gas phase. Bulk solvation, however, influences the rate of C3′−O(P) bond breakage to become faster than that of glycosidic bond rupture.

C3′−O(P) bond breakage in **•UH** has a barrier in the gas phase of 10.7 kcal mol^{-1}; 8.2 kcal mol^{-1} when including ZPE correction. Thermal corrections at 298 K leads to a lowering of the barrier to 6.8 kcal mol^{-1}. Bulk solvation, however, is unfavorable to the bond dissociation and results in a barrier that is 2.1 kcal mol^{-1} higher than that in the gas phase. Notably, the reaction energy and corresponding free energy is −28.7 kcal mol^{-1} and −31.4 kcal mol^{-1}, respectively. Removing the possibility of O2′−H2′···O(P) hydrogen bonding contributes to a reduction in the barrier by only 1 kcal mol^{-1}.

Compared with the corresponding data for **•U**, it seems clear that the protonation state of the phosphate group influences the dynamic process and thermodynamic properties of the C3′–O(P) breakage reaction.

The differences between **•U** and **•UH** can be attributed to their respective transition structures (see Figure 2). C3′–O(P) bond breakage of **•UH** is the most facile of all reactions studied herein. The computed barrier height is in agreement with the 7.06 (3′dTMPH) and 11.6 kcal mol^{-1} (5′dTMPH) reported by Gu et al.[25] and 11.6 kcal mol^{-1} (5′dTMPH) by Kumar and Sevilla.[33]

Changes in Mulliken charges and unpaired spin density along the dissociation processes: To determine the electronic properties along the bond-dissociation processes, the changes of total Mulliken charges and unpaired spin density in each separate fragment are estimated in the gas phase through the relaxed PES scans. The resulting data for the separate fragments are displayed in Figure 4.

For the initial reactants, the charges are mainly found on the phosphate group of **•U** and on the uracil base of **•UH**. In the process of glycosidic bond rupture in **•U** and **•UH**, the charges on the uracil base increase drastically with increasing C1′···N1 distance and are then transferred to the ribose + phosphate fragment after the transition states. In the transition states, the smallest charges are found on the uracil bases. The charges are completely localized on the ribose in the final products. The changes in unpaired spin density on the uracil base are very similar. Before the transition states, the spin densities on the uracil bases are relatively constant, which is then followed by a steep decrease close to the transition state. This change is in agreement with that of the total negative charges on the base. Hence, both charge separation and spin transfer within the two fragments are factors contributing to the glycosidic bond rupture.

In the dissociation process of the C3′–O(P) bond of **•U** and **•UH**, the negative charge on the phosphate group increases steadily with increased C3′···O(P) distance. At the transition states, the partial negative charges are transferred to ribose from the phosphate in **•U** and from the uracil base to ribose in **•UH**. In the final dissociation products, the total charges are averaged out between the phosphate and the uracil + ribose fragments of **UP-CO**, whereas it resides mainly on the phosphate in **UHP-CO**. The unpaired spin changes very little before the transition states. Near the transition structures, they sharply increase, and then decrease with increased C3′···O(P) distance. Thus, charge and spin transfer are also considered as important factors for C3′–O(P) bond rupture.

Conclusions

In the present work, hybrid DFT methodology has been employed to investigate the N1-glycosidic and C3′–O(P) bond-breakage processes induced by electron addition to 3′UMP and the protonated 3′UMPH. Geometries, ZPE and thermal corrections at $T=298$ K, Mulliken charges, unpaired spin

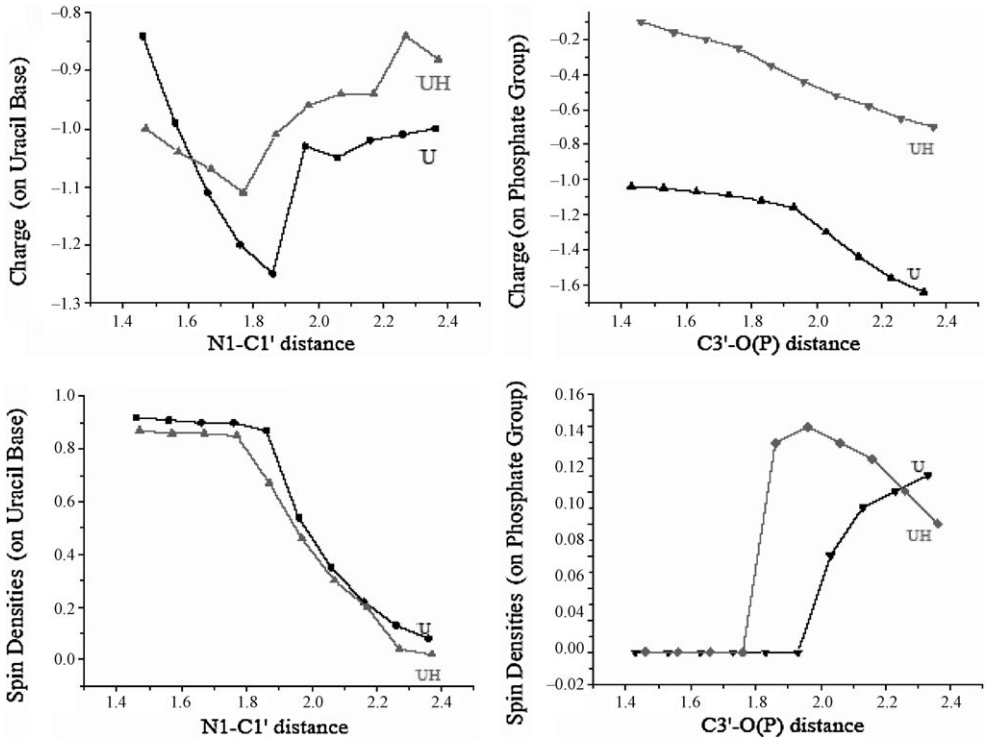

Figure 4. Mulliken charge populations (top row) and spin density surfaces (bottom row) along the N1-glycosidic (left side) and C3′–O(P) (right side) bond-breakage reactions of **•U** (a) and **•UH** (b).

densities, and reaction energies were obtained at the B3LYP/6-31+G(d,p) level in the gas phase. This was followed by single-point calculations performed at the same level in aqueous solution ($\varepsilon = 78.4$) by using the IEF-PCM model.

The values of VEA, AEA of **U**, and VDE of **$^{\bullet}$U** are negative in the gas phase but become positive upon inclusion of bulk solvation. **$^{\bullet}$UH** has positive VDE values already in the gas phase, which shows that the electron adducts can be stable in both media. Both glycosidic and C3′−O(P) bond-dissociation processes are found to be feasible, but the protonation state of phosphate, the C2′−OH group, and bulk solvation play significant, and different, roles in the two systems: First, the processes of glycosidic bond dissociation in **$^{\bullet}$U** and **$^{\bullet}$UH** are exothermic with high barrier heights in the gas phase. Bulk solvation reduces the barriers to around 20 kcal mol^{-1}. The charge state on the phosphate does not influence the barrier heights and reaction energies significantly, whereas the presence of the C2′−OH group in ribose raises the barriers compared with deoxyribose. This is especially striking in the case of the glycosidic bond dissociation of **$^{\bullet}$UH**. Second, for C3′−O(P) bond dissociation in **$^{\bullet}$U** and **$^{\bullet}$UH**, a high barrier is found for **$^{\bullet}$U** in the gas phase along with a strongly endothermic overall process. Bulk solvation reduces the barrier to 14.7 kcal mol^{-1} and the reaction energy to 1.0 kcal mol^{-1}. The C2′−OH group stabilizes the transition structure of **$^{\bullet}$U** significantly, which slightly disfavors the transition structure of **$^{\bullet}$UH** in gas phase. The protonation state on phosphate is crucial to the C3′−O(P)-bond dissociation and the reaction energy. The C3′−O(P) bond rupture of **$^{\bullet}$UH** is the most facile of all the investigated reactions, which is similar to the findings of Gu et al. on related systems.[25,27]

Third, the changes in Mulliken charges and unpaired spin distribution play major roles in the dissociation of the glycosidic bond in both **$^{\bullet}$U** and **$^{\bullet}$UH**. In addition, unpaired spin transfer favors C3′−O(P) bond dissociation in **$^{\bullet}$U** and **$^{\bullet}$UH**, in particular in **$^{\bullet}$UH**.

Acknowledgements

The Swedish science research council (VR) and the National Science Foundation of China (grant number 20643007) are gratefully acknowledged for financial support. We also acknowledge generous grants of computing time at the National supercomputing facilities in Linköping (NSC).

[1] Z. Cai, M. D. Sevilla, *Top. Curr. Chem.* **2004**, *237*, 103.
[2] C. von Sonntag, *Free-Radical-Induced DNA Damage and Its Repair*, Springer, Berlin, **2006**, p. 82, p. 213.
[3] J. A. LaVerne, S. M. Pimblott, *Radiat. Res.* **1995**, *141*, 208.
[4] B. Boudaiffa, P. Cloutier, D. Hunting, M. A. Huels, L. Sanche, *Science* **2000**, *287*, 1658.
[5] M. A. Huels, B. Boudaiffa, P. Cloutier, D. Hunting, L. Sanche, *J. Am. Chem. Soc.* **2003**, *125*, 4467.
[6] Y. Zheng, P. Cloutier, D. J. Hunting, J. R. Wagner, L. Sanche, *J. Am. Chem. Soc.* **2004**, *126*, 1002.
[7] Y. Zheng, P. Cloutier, D. J. Hunting, L. Sanche, J. R. Wagner, *J. Am. Chem. Soc.* **2005**, *127*, 16592.
[8] F. Martin, P. D. Burrow, Z. Cai, P. Cloutier, D. Hunting, L. Sanche, *Phys. Rev. Lett.* **2004**, *93*, 068101.
[9] G. Hanel, S. Denifl, P. Scheier, M. Probst, B. Farizon, M. Farizon, E. Illenberger, T. D. Mark, *Phys. Rev. Lett.* **2003**, *90*, 188104.
[10] H. Abdoul-Carime, S. Gohlke, E. Illenberger, *Phys. Rev. Lett.* **2004**, *92*, 168103.
[11] S. Denifl, S. Ptasiñska, M. Cingel, S. Matejcik, P. Scheier, T. D. Mark, *Chem. Phys. Lett.* **2003**, *377*, 74.
[12] R. Abouaf, J. Pommier, H. Dunet, *Int. J. Mass Spectrom.* **2003**, *226*, 397.
[13] S. Ptasiñska, S. Denifl, P. Scheier, E. Illenberger, T. D. Mark, *Angew. Chem.* **2005**, *117*, 7101; *Angew. Chem. Int. Ed.* **2005**, *44*, 6941.
[14] I. Bald, J. Kopyra, E. Illenberger, *Angew. Chem.* **2006**, *118*, 4969; *Angew. Chem. Int. Ed.* **2006**, *45*, 4851.
[15] C. Konig, J. Kopyra, I. Bald, E. Illenberger, *Phys. Rev. Lett.* **2006**, *97*, 018105.
[16] S. Denifl, S. Ptasiñska, M. Probst, J. Hrusak, P. Scheier, T. D. Mark, *J. Phys. Chem. A* **2004**, *108*, 6562.
[17] S. Ptasiñska, S. Denifl, B. Mroz, M. Probst, V. Grill, E. Illenberger, P. Scheier, T. D. Mark, *J. Chem. Phys.* **2005**, *123*, 124302.
[18] R. Barrios, P. Skurski, J. Simons, *J. Phys. Chem. B* **2002**, *106*, 7991.
[19] J. Berdys, I. Anusiewicz, P. Skurski, J. Simons, *J. Phys. Chem. A* **2004**, *108*, 2999.
[20] J. Berdys, P. Skurski, J. Simons, *J. Phys. Chem. B* **2004**, *108*, 5800.
[21] I. Anusiewicz, J. Berdys, M. Sobczyk, P. Skurski, J. Simons, *J. Phys. Chem. A* **2004**, *108*, 11381.
[22] J. Berdys, I. Anusiewicz, P. Skurski, J. Simons, *J. Am. Chem. Soc.* **2004**, *126*, 6441.
[23] J. Simons, *Acc. Chem. Res.* **2006**, *39*, 772.
[24] X. Li, M. D. Sevilla, L. Sanche, *J. Am. Chem. Soc.* **2003**, *125*, 13668.
[25] J. Gu, Y. Xie, H. F. Schaefer, *J. Am. Chem. Soc.* **2005**, *127*, 1053.
[26] X. Bao, J. Wang, J. Gu, J. Leszczynski, *Proc. Natl. Acad. Sci. USA* **2006**, *103*, 5658.
[27] J. Gu, J. Wang, J. Leszczynski, *J. Am. Chem. Soc.* **2006**, *128*, 9322.
[28] J. Gu, Y. Xie, H. F. Schaefer, *J. Am. Chem. Soc.* **2006**, *128*, 1250.
[29] J. Gu, Y. Xie, H. F. Schaefer, *J. Phys. Chem. B* **2006**, *110*, 19696.
[30] X. Li, M. D. Sevilla, L. Sanche, *J. Phys. Chem. B* **2004**, *108*, 19013.
[31] X. Li, M. D. Sevilla, *Adv. Quantum Chem.* **2007**, *52*, 59.
[32] X. Li, L. Sanche, M. D. Sevilla, *Radiat. Res.* **2006**, *165*, 721.
[33] A. Kumar, M. D. Sevilla, *J. Phys. Chem. B* **2007**, *111*, 5464.
[34] E. Westhof, *Science* 1999, 286, 61.
[35] A. D. Becke, *J. Chem. Phys.* **1993**, *98*, 5648.
[36] C. Lee, W. Yang, R. G. Parr, *Phys. Rev. B* **1988**, *37*, 785.
[37] J. Tomasi, M. Persico, *Chem. Rev.* **1994**, *94*, 2027.
[38] M. J. Frisch, G. W. Trucks, H. B. Schlegel, G. E. Scuseria, M. A. Robb, J. R. Cheeseman, J. A. Montgomery Jr., T. Vreven, K. N. Kudin, J. C. Burant, J. M. Millam, S. S. Iyengar, J. Tomasi, V. Barone, B. Mennucci, M. Cossi, G. Scalmani, N. Rega, G. A. Petersson, H. Nakatsuji, M. Hada, M. Ehara, K. Toyota, R. Fukuda, J. Hasegawa, M. Ishida, T. Nakajima, Y. Honda, O. Kitao, H. Nakai, M. Klene, X. Li, J. E. Knox, H. P. Hratchian, J. B. Cross, C. Adamo, J. Jaramillo, R. Gomperts, R. E. Stratmann, O. Yazyev, A. J. Austin, R. Cammi, C. Pomelli, J. W. Ochterski, P. Y. Ayala, K. Morokuma, G. A. Voth, P. Salvador, J. J. Dannenberg, V. G. Zakrzewski, S. Dapprich, A. D. Daniels, M. C. Strain, O. Farkas, D. K. Malick, A. D. Rabuck, K. Raghavachari, J. B. Foresman, J. V. Ortiz, Q. Cui, A. G. Baboul, S. Clifford, J. Cioslowski, B. B. Stefanov, G. Liu, A. Liashenko, P. Piskorz, I. Komaromi, R. L. Martin, D. J. Fox, T. Keith, M. A. Al-Laham, C. Y. Peng, A. Nanayakkara, M. Challacombe, P. M. W. Gill, B. Johnson, W. Chen, M. W. Wong, C. Gonzalez, J. A. Pople, *Gaussian 03*, Revision B.04, Gaussian, Inc.: Pittsburgh, PA, **2003**.
[39] J. C. Rienstra-Kiracofe, G. S. Tschumper, H. F. Schaefer, S. Nandi, G. B. Ellison, *Chem. Rev.* **2002**, *102*, 231.
[40] S. D. Wetmore, R. J. Boyd, L. A. Eriksson, *Chem. Phys. Lett.* **2000**, *322*, 129.

Received: August 25, 2007
Published online: January 21, 2008

